ETH
Eidgenössische Technische Hochschule Zürich
Swiss Federal Institute of Technology Zurich

Seminar for Applied Mathematics SAM

# Robust finite difference schemes for a nonlinear variational wave equation modeling liquid crystals

F. Weber

Research Report No. 2013-43

November 2013
Latest revision: May 2016

Seminar für Angewandte Mathematik
Eidgenössische Technische Hochschule
CH-8092 Zürich
Switzerland

Funding ERC: StG 306279 SPARCCLE

# ROBUST FINITE DIFFERENCE SCHEMES FOR A NONLINEAR VARIATIONAL WAVE EQUATION MODELING LIQUID CRYSTAL DYNAMICS

FRANZISKA WEBER

Abstract. We consider a nonlinear variational wave equation that models the dynamics of nematic liquid crystals. Finite difference schemes that either conserve or dissipate a discrete version of the energy associated with these equations are designed. Numerical experiments in one and two-space dimensions illustrating the stability and efficiency of the schemes are presented. An interesting feature of these schemes is their ability to approximate both the conservative as well as the dissipative weak solutions of the underlying system.

## 1. Introduction

1.1. **The model.** The dynamics of nematic liquid crystals is an important object of study in both physics and engineering. Many popular models of nematic liquid crystals consider a medium consisting of thin rods that are allowed to rotate about their center of mass but are not allowed to translate. Under the assumption that the medium is not flowing and deformations only occur when the mean orientation of the long molecules is changed, one can describe the orientation of the molecules at each location $\mathbf{x} \in \mathbb{R}^3$ and time $t \in \mathbb{R}$ using a field of unit vectors

$$\mathbf{n} = \mathbf{n}(\mathbf{x}, t) \in \mathcal{S}^2.$$

This field $\mathbf{n}$ is termed as the *director field*.

Given a director field $\mathbf{n}$, the well-known Oseen-Frank potential energy density $\mathbf{W}$ associated with this field, is given by

$$\mathbf{W}(\mathbf{n}, \nabla\mathbf{n}) = \alpha \left|\mathbf{n} \times (\nabla \times \mathbf{n})\right|^2 + \beta \left(\nabla \cdot \mathbf{n}\right)^2 + \gamma \left(\mathbf{n} \cdot (\nabla \times \mathbf{n})\right)^2. \tag{1.1}$$

The positive constants $\alpha, \beta$ and $\gamma$ are the elastic constants of the liquid crystal. Note that each term on the right hand side of (1.1) arises from different types of distortions. For instance, the term $\alpha \left|\mathbf{n} \times (\nabla \times \mathbf{n})\right|^2$ corresponds to the bending of the medium, the term $\beta \left(\nabla \cdot \mathbf{n}\right)^2$ corresponds to a type of deformation called splay, and the term $\gamma \left(\mathbf{n} \cdot (\nabla \times \mathbf{n})\right)^2$ corresponds to the twisting of the medium.

For the special case of $\alpha = \beta = \gamma$, the potential energy density (1.1) reduces to

$$\mathbf{W}(\mathbf{n}, \nabla\mathbf{n}) = \alpha \left|\nabla\mathbf{n}\right|^2,$$

which corresponds to the potential energy density for harmonic maps into the sphere $\mathcal{S}^2$. The constrained elliptic system of equations for $\mathbf{n}$ derived from the potential (1.1) using a variational principle and the parabolic flow associated with it, have been extensively studied, see [1, 9, 11] and references therein. In this article, we will focus on the equations modeling the dynamics in the regime where inertial effects dominate over viscosity. Inertial effects become important when the director field is subject to large accelerations [19] or high frequency excitations on small time scales [2]. Other applications include acoustics [22] and models of liquid crystals under the influence of mechanical vibrations [26].

*Date*: May 17, 2016.

2010 *Mathematics Subject Classification.* 65M06, 35L70, 65M12.

*Key words and phrases.* Nonlinear variational wave equation, energy preserving scheme, finite difference method.

The author wishes to thank Siddhartha Mishra, Ujjwal Koley and Nils Henrik Risebro for helpful discussions and useful advice on the subject.

In this regime, it is more natural to model the propagation of orientation waves in the director field by employing the principle of least action [23], that is,

$$\frac{\delta}{\delta \mathbf{n}} \iint \left(\mathbf{n}_t^2 - \mathbf{W}(\mathbf{n}, \nabla \mathbf{n})\right)\, dx\, dt = 0, \qquad \mathbf{n}\cdot\mathbf{n} = 1. \tag{1.2}$$

Again in the special case where $\alpha = \beta = \gamma$, this variational principle (1.2) yields the equation for harmonic wave maps from the $(1+3)$-dimensional Minkowski space into the 2-sphere, see [8, 24, 25] and references therein.

1.1.1. *One-dimensional planar waves.* Planar deformations are of great interest in the study of nematic liquid crystals. In particular, if we assume that the deformation depends on a single space variable $x$ and that it varies only in the $(x,y)$–plane, the director field $\mathbf{n}$ has the form

$$\mathbf{n} = \cos u(x,t)\mathbf{e}_x + \sin u(x,t)\mathbf{e}_y.$$

Here, the unknown $u \in \mathbb{R}$ measures the angle of the director field to the $x$-direction, and $\mathbf{e}_x$ and $\mathbf{e}_y$ are the coordinate vectors in the $x$ and $y$ directions, respectively. In this case, the Euler-Lagrange equations of the variational principle (1.2) reduce to

$$\begin{aligned} u_{tt} - c(u)\left(c(u)u_x\right)_x = 0, &\quad (x,t) \in \Pi_T, \\ u(x,0) = u_0(x), &\quad x \in \mathbb{R}, \\ u_t(x,0) = u_1(x), &\quad x \in \mathbb{R}, \end{aligned} \tag{1.3}$$

where $\Pi_T = \mathbb{R}\times[0,T]$ with fixed $T > 0$ , and the wave speed $c(u)$ given by

$$c^2(u) = \alpha\cos^2 u + \beta \sin^2 u, \tag{1.4}$$

for some positive constants $\alpha, \beta$. The form (1.3) is the standard form of the nonlinear variational wave equation considered in the literature, [7, 27, 23, 12, 14].

If we consider the following *energy*:

$$\mathcal{E}(t) = \int_{\mathbb{R}} \left(u_t^2 + c^2(u)u_x^2\right)\, dx, \tag{1.5}$$

a simple calculation shows that smooth solutions of the variational wave equation (1.3) *conserve* this energy, that is, they satisfy

$$\frac{d\mathcal{E}(t)}{dt} \equiv 0. \tag{1.6}$$

1.1.2. *Two-dimensional planar waves.* Similarly, if the planar deformation depends on two space variables $x, y$, the director field has the form

$$\mathbf{n} = \cos u(x,y,t)\mathbf{e}_x + \sin u(x,y,t)\mathbf{e}_y,$$

with $u$ being the angle to the $(x,y)$–plane. The corresponding wave equation is given by,

$$\begin{aligned} u_{tt} - c(u)\left(c(u)u_x\right)_x - b(u)\left(b(u)u_y\right)_y - a'(u)u_xu_y - 2a(u)u_{xy} = 0, &\quad (x,y,t) \in \mathbb{Q}_T, \\ u(x,y,0) = u_0(x,y), &\quad (x,y) \in \mathbb{R}^2, \\ u_t(x,y,0) = u_1(x,y), &\quad (x,y) \in \mathbb{R}^2, \end{aligned} \tag{1.7}$$

where $\mathbb{Q}_T = \mathbb{R}^2\times[0,T]$ with $T > 0$ fixed, $u : \mathbb{Q}_T \to \mathbb{R}$ is the unknown function and $a, b, c$ are given by

$$\begin{aligned} c^2(u) &= \alpha\cos^2 u + \beta\sin^2 u, \\ b^2(u) &= \alpha\sin^2 u + \beta\cos^2 u, \\ a(u) &= \frac{\alpha-\beta}{2}\sin(2u). \end{aligned}$$

for some constants $\alpha$ and $\beta$. Furthermore, smooth solutions of (1.7) conserve the following energy:

$$\begin{aligned}\mathcal{E}(t) &= \iint_{\mathbb{R}^2} \left(u_t^2 + c^2(u)u_x^2 + b^2(u)u_y^2 + 2a(u)u_xu_y\right)\,dx\,dy \\ &= \iint_{\mathbb{R}^2} \left(u_t^2 + \alpha(\cos(u)u_x + \sin(u)u_y)^2 + \beta(\sin(u)u_x - \cos(u)u_y)^2\right)\,dx\,dy,\end{aligned} \tag{1.8}$$

that is, smooth solutions satisfy (1.6) with respect to the above energy.

1.2. **Mathematical issues.** Even though the nonlinear variational wave equation does not capture all physical effects, it does model interesting physical behavior and has interesting mathematical properties. It is well known that the solution of the initial value problem, even for the one-dimensional planar wave equation (1.3) develops singularities in finite time, even if the initial data are smooth [13]. Hence, solutions of (1.3) are defined in the sense of distributions:

**Definition 1.1.** *Let $\Pi_T = \mathbb{R}\times(0,T)$. A function*

$$u(t,x) \in L^\infty\left([0,T];W^{1,p}(\mathbb{R})\right)\cap C(\Pi_T), u_t \in L^\infty\left([0,T];L^p(\mathbb{R})\right),$$

*for all $p\in[1,3+q]$, where $q$ is some positive constant, is a weak solution of the initial value problem (1.3) if it satisfies:*

*(1) For all test functions $\varphi\in\mathcal{D}(\mathbb{R}\times[0,T))$,*

$$\iint_{\Pi_T}\left(u_t\varphi_t - c^2(u)u_x\varphi_x - c(u)c'(u)(u_x)^2\varphi\right)\,dx\,dt = 0. \tag{1.9}$$

*(2) $u(\cdot,t)\to u_0$ in $C\left([0,T];L^2(\mathbb{R})\right)$ as $t\to 0^+$.*

*(3) $u_t(\cdot,t)\to v_0$ as a distribution in $\Pi_T$ when $t\to 0^+$.*

It is highly non-trivial to extend the solution after the appearance of singularities. In particular, the choice of this extension is not unique. Two distinct types of solutions, the so-called *conservative* and *dissipative* solutions are known. To illustrate this difference, one considers initial data for which the solution vanishes identically at some specific (finite) time. At this point, at least two possibilities exist: to continue with the trivial zero solution termed as the dissipative solution. As an alternative, one can show that there exists a nontrivial solution that appears as a natural continuation of the solution after the critical time. This solution is denoted the conservative solution as it preserves the total energy of the system. This dichotomy makes the question of well-posedness of the initial value problem (1.3) very difficult. Additional admissibility conditions are needed to select a physically relevant solution. The specification of such admissibility criteria is still an open question.

Although the problem of global existence and uniqueness of solutions to the Cauchy problem of the nonlinear variational wave equation (1.3) is still open, several recent papers have explored related questions or particular cases of (1.3). It has been demonstrated in [14] that (1.3) is rich in structural phenomena associated with weak solutions. In fact, rewriting the highest derivatives of (1.3) in conservative form

$$u_{tt} - \left(c^2(u)u_x\right)_x = -c(u)c'(u)u_x^2,$$

we see that the strong precompactness in $L^2$ of the derivatives $\{u_x\}$ of a sequence of approximate solutions is essential in establishing the existence of a global weak solution. However, the equation shows the phenomenon of persistence of oscillations [10] and annihilation in which a sequence of exact solutions with bounded energy can oscillate forever so that the sequence $\{u_x\}$ is not precompact in $L^2$, but the weak limit of the sequence is still a weak solution.

There has been a number of papers concerned with the existence of weak solutions of the Cauchy problem (1.3), starting with the papers by Zhang and Zheng [27, 29, 28, 30, 32, 31], Bressan and Zheng [7] and Holden *et al.* [17]. In [32], the authors show existence of a global weak solution, using method of Young measures, for initial data $u_0\in H^1(\mathbb{R})$ and $u_1\in L^2(\mathbb{R})$. The function $c$ is assumed to be smooth, bounded, positive with derivative that is non-negative and strictly positive

on the initial data $u_0$. This means that the analysis in [17, 27, 29, 28, 30, 32, 31] does not directly apply to (1.3).

A different approach to the study of (1.3) was taken by Bressan and Zheng in [7]. Here, they rewrite the equation in new coordinates such that the singularities disappear. They show that for $u_0$ absolutely continuous with $(u_0)_x, u_1 \in L^2(\mathbb{R})$, the Cauchy problem (1.3) allows a global weak solution with the following properties: the solution $u$ is locally Lipschitz continuous and the map $t \to u(t,\cdot)$ is continuously differentiable with values in $L^p_{\text{loc}}(\mathbb{R})$ for $1 \leq p < 2$.

In [17], Holden and Raynaud prove the existence of a global semigroup for conservative solutions of (1.3), allowing for concentration of energy density on sets of zero measure. Furthermore they also allow for initial data $u_0, u_1$ that contain measures. The proof involves constructing the solution by introducing new variables related to the characteristics, leading to a characterization of singularities in the energy density. They also prove that energy can only focus on a set of times of zero measure or at points where $c'(u)$ vanishes.

In contrast to the one-dimensional case, hardly any rigorous wellposedness or even qualitative results are available for the two-dimensional version of the variational wave equation (1.7).

1.3. **Numerical schemes.** Given the nonlinear nature of the variational wave equations (1.3) and (1.7), explicit solution formulae are hard to obtain. Consequently, robust numerical schemes for approximating the variational wave equation are very important in the study of nematic liquid crystals. However, there is a paucity of efficient numerical schemes for these equations. Within the existing literature, we can refer to [12], where the authors present some numerical examples to illustrate their theory. Recently, a semi-discrete finite difference scheme for approximating one-dimensional equation (1.3) was considered in [16]. The authors were even able to prove convergence of the numerical approximation, generated by their scheme, to the *dissipative* solutions of (1.3). However, the underlying assumptions on the wave speed $c$ (positivity of the derivative of $c$) precludes consideration of realistic wave speeds given by (1.4). Another recent paper dealing with the numerical approximation of (1.3) is [17], where the authors use an analytical construction to define a numerical method that can approximate the *conservative* solution. However, the method is computationally very expensive as there is no time marching.

Besides the above mentioned results, there has been done work on numerical methods for the Ericksen–Leslie (EL) equations [4] (essentially the simplest set of equations describing the motion of a nematic liquid crystal). In [6], the authors present a finite element scheme for the EL equations. Their numerical method is based on the ideas given in [5] which utilizes the Galerkin method with Lagrange finite elements of order 1. Convergence, even to measure-valued solutions, of such schemes is an open problem. In [3], a saddle-point formulation is used to construct finite element approximations to the EL equations.

A penalty method based on well-known penalty formulation for the EL equations has been introduced in [20], it uses the *Ginzburg–Landau* approach. Convergence of such approximate solutions, based on an energy method and a compactness result, towards measure valued solutions has been proved in [21].

1.4. **Aims and scope of the current paper.** The above discussion clearly highlights the lack of robust and efficient numerical schemes to simulate the nonlinear variational wave equation (1.3). In particular, one needs a scheme that is both efficient and simple to implement, and able to approximate the solutions of (1.3) accurately. Furthermore, one can expect both *conservative* as well as *dissipative* solutions of the variational wave equation (1.3) after singularity formation. Hence, it is essential to design schemes that approximate these different types of solutions.

To this end, we will construct robust finite difference schemes for approximating the variational wave equation in both one and two space dimensions. The key design principle will be energy conservation (dissipation). As pointed out before, smooth solutions of (1.3) and (1.7) are energy conservative. After singularity formation, this energy is either conserved or dissipated. We will design numerical schemes that imitate this energy principle. In other words, our schemes will either conserve a discrete form of the energy (1.5) or dissipative it. This way, we construct schemes that approximate the conservative and the dissipative solutions in both, one and two space dimensions.

Extensive numerical experiments are presented to illustrate that the energy conservative (dissipative) schemes converge to the conservative (dissipative) solution of the variational wave equation as the mesh is refined. To the best of our knowledge, these are the first fully discrete finite difference schemes that can approximate the conservative solutions of the one-dimensional variational wave equation. Furthermore, we present the first set of numerical schemes to approximate the two-dimensional version of these equations. Our energy conservative (dissipative) schemes are based on rewriting the wave equation as a first-order system of equations. Due to the nonlinearity and the lack of existence of a conservative formulation for the equations, proving convergence for time marching schemes approximating the variational wave equations is difficult. To the best of our knowledge, for finite difference schemes, this has only been obtained under certain non-physical constraints such as, as mentionned previously, the one-constant approximation [18], or monotone wave speeds for semi-discrete schemes [16].

The rest of the paper is organized as follows: In Section 2, we present energy conservative and energy dissipative schemes for the one-dimensional equation (1.3). Numerical experiments illustrating these schemes are presented in Section 3. The two-dimensional schemes are presented in Section 4.

## 2. Numerical schemes for the one-dimensional variational wave equation (1.3)

2.1. **The grid and notation.** We first introduce some notation needed to define the finite difference schemes. Throughout this paper, we reserve $h$ and $\Delta t$ to denote two small positive numbers that represent the spatial and temporal discretization parameters, respectively, of the numerical schemes. For $j \in \mathbb{N}_0 = \mathbb{N} \cup \{0\}$, we set $x_j = jh$, and for $n = 0, 1, ..., N$, where $N\Delta t = T$ for some fixed time horizon $T > 0$, we set $t_n = n\Delta t$. For any function $g = g(x)$, we write $g_j = g(x_j)$, and similarly for any function $g = g(x, t)$, we write $g_j^n = g(x_j, t_n)$. We also introduce the spatial and temporal grid cells

$$I_j = [x_{j-\frac{1}{2}}, x_{j+\frac{1}{2}}), \qquad I_j^n = I_j \times [t_n, t_{n+1}).$$

Furthermore we introduce the difference operators,

$$D^{\pm}\rho_j = \pm\frac{\rho_{j\pm1} - \rho_j}{h}, \quad D^0\rho_j = \frac{1}{2}\left(D^+ + D^-\right)\rho_j, \quad D_t\rho^n = \frac{\rho^{n+1} - \rho^n}{\Delta t}.$$

2.2. **A first-order system for (1.3).** It is easy to check that at the formal level, the variational wave equation (1.3) can be rewritten as a first-order system by introducing the independent variables:

$$\begin{aligned} v &:= u_t \\ w &:= c(u)u_x. \end{aligned}$$

Then, for smooth solutions, equation (1.3) is equivalent to the following system for $(v, w, u)$,

$$\begin{cases} v_t - c(u)w_x = 0 \\ w_t - (c(u)v)_x = 0, \\ u_t = v. \end{cases} \tag{2.1}$$

The energy associated with the above equation is

$$\mathcal{E}(t) = \frac{1}{2}\int_{\mathbb{R}} \left(v^2 + w^2\right) dx. \tag{2.2}$$

One can check that smooth solutions of (2.1) preserve this energy. Weak solutions can be either energy conservative or energy dissipative.

2.3. **Energy preserving scheme based on system (2.1).** Our objective is to design a finite difference scheme such that the numerical approximations conserve a discrete version of the energy (2.2). To this end, we suggest the following finite difference scheme:

$$\begin{aligned}(v_j)_t - c_j D^0 w_j &= 0,\\ (w_j)_t - D^0\left(c_j v_j\right) &= 0,\\ (u_j)_t &= v_j.\end{aligned} \tag{2.3}$$

The energy conservation property of this semi-discrete scheme is presented in the following lemma:

**Lemma 2.1.** *Let $v_j(t)$ and $w_j(t)$ be approximate solutions generated by the scheme (2.3). Then*

$$\frac{d}{dt}\left(\frac{h}{2}\sum_j (v_j^2(t)+w_j^2(t))\right) = 0.$$

*Proof.* To prove this lemma, one multiplies the first equation in (2.3) by $v_j$ and second equation by $w_j$ respectively. Then using chain rule for the time derivatives, adding up the two equations and summing over all $j$, one has (omitting the time dependence of the variables)

$$\frac{1}{2}\frac{d}{dt}\sum_j \left(v_j^2+w_j^2\right) = \sum_j \left(v_j c_j D^0 w_j + w_j D^0(c_j v_j)\right).$$

Relabeling the indices and using the boundary conditions, one sees that the right hand side of the above equation is equal to zero.

□

2.4. **Energy dissipating scheme based on system (2.1).** We expect the above designed energy conservative scheme (2.3) to approximate a conservative solution of the underlying system (1.3). In order to be able to approximate a dissipative solution of (1.3), we propose the following modification of the energy conservative scheme (2.3):

$$\begin{aligned}(v_j)_t - c_j D^0 w_j &= \frac{h}{2} D^-\left(s_{j+\frac{1}{2}} D^+ v_j\right)\\ (w_j)_t - D^0\left(c_j v_j\right) &= \frac{h}{2} D^-\left(s_{j+\frac{1}{2}} D^+ w_j\right),\\ (u_j)_t &= v_j,\end{aligned} \tag{2.4}$$

where we have chosen $s_{j\pm\frac{1}{2}} = \max\{c_j, c_{j\pm1}\}$ i.e, the maximum local wave speed.

We show that the above scheme dissipates energy in the following lemma:

**Lemma 2.2.** *Let $v_j(t)$ and $w_j(t)$ be approximate solutions generated by the scheme (2.4). Then one can prove that*

$$\frac{d}{dt}\left(\frac{h}{2}\sum_j (v_j^2(t)+w_j^2(t))\right) \le 0,$$

*with strict inequality if $w$ or $v$ is not constant.*

*Proof.* As in Lemma 2.1, we multiply the first equation of 2.4 by $v_j$ and the second by $w_j$, use chain rule for the time derivatives, add the two equations and sum over all indices $j$. We obtain

$$\begin{aligned}\frac{1}{2}\frac{d}{dt}\sum_j \left(v_j^2+w_j^2\right) =& \sum_j \left(v_j c_j D^0 w_j + w_j D^0(c_j v_j)\right)\\ &+ \frac{h}{2}\sum_j \left(v_j D^-\left(s_{j+\frac{1}{2}} D^+ v_j\right) + w_j D^-\left(s_{j+\frac{1}{2}} D^+ w_j\right)\right).\end{aligned}$$

As before, the first term on the right hand side is zero, using the boundary conditions. For the second term, we rename the indices in the sums, and use the boundary condition to obtain that it is equal to

$$\frac{h}{2}\sum_j \left(v_j D^-\left(s_{j+\frac{1}{2}} D^+ v_j\right) + w_j D^-\left(s_{j+\frac{1}{2}} D^+ w_j\right)\right) = -\frac{h}{2}\sum_j \left(s_{j+\frac{1}{2}}\left(D^+ v_j\right)^2 + s_{j+\frac{1}{2}}\left(D^+ w_j\right)^2\right).$$

Since $s_{j+\frac{1}{2}} \geq 0$ for all $j$, the right hand side is nonpositive and the claim follows. □

Hence, the scheme (2.4) is energy stable (dissipating) and we expect it to converge to a dissipative solution of (1.3) as the mesh is refined. We remark that energy dissipation results from adding *numerical viscosity* (scaled by the maximum wave speed) to the energy conservative scheme (2.3).

**Remark 2.1.** *Note that upwinding is a more standard way of obtaining stability, especially for nonlinear hyperbolic conservation laws. However, for this model, our particular choice of symmetric fluxes is precisely what gives the conservative (energy preserving) scheme. For the dissipative scheme our choice can be seen as a type of upwinding.*

2.5. **A first-order system for (1.3) based on Riemann invariants.** We can also rewrite the one-dimensional variational wave equation (1.3) as a first-order system of equations by introducing the Riemann invariants:

$$R := u_t + c(u)u_x$$
$$S := u_t - c(u)u_x.$$

Again, for smooth solutions, equation (1.3) is equivalent to the following system in non-conservative form for $(R, S, u)$,

$$\begin{cases} R_t - c(u)R_x = \frac{c'(u)}{4c(u)}\left(R^2 - S^2\right), \\ S_t + c(u)S_x = -\frac{c'(u)}{4c(u)}\left(R^2 - S^2\right), \\ u_t = \frac{R+S}{2}. \end{cases} \tag{2.5}$$

Observe that one can also rewrite the equation (1.3) in conservative form for $(R, S, u)$,

$$\begin{cases} R_t - (c(u)R)_x = -\frac{c_x(u)}{2}\left(R - S\right), \\ S_t + (c(u)S)_x = -\frac{c_x(u)}{2}\left(R - S\right), \\ u_t = \frac{R+S}{2}. \end{cases} \tag{2.6}$$

The corresponding energy associated with the system (2.5) is

$$\mathcal{E}(t) = \frac{1}{4}\int_{\mathbb{R}} \left(R^2 + S^2\right) dx. \tag{2.7}$$

A simple calculation shows that smooth solutions of (2.5) satisfy the energy identity:

$$(R^2 + S^2)_t - \left(c(u)(R^2 - S^2)\right)_x = 0. \tag{2.8}$$

Hence, the fact that the total energy (2.7) is conserved follows from integrating the above identity in space and assuming that the functions $R, S$ decay at infinity.

2.6. **Energy preserving scheme based on the Riemann invariants formulation.** To obtain the formal energy identity (2.8), one needs to use the chain rules

$$c(u)RR_x = \frac{1}{2}c(u)\left(R^2\right)_x, \quad c(u)SS_x = \frac{1}{2}c(u)\left(S^2\right)_x.$$

In the setting of finite differences, such an identity is not possible. Therefore we base our scheme on the following reformulation of (2.6),

$$\begin{cases} R_t - \frac{1}{2}(c(u)R)_x = \frac{1}{2}\left(c_x(u)S + c(u)R_x\right), \\ S_t + \frac{1}{2}(c(u)S)_x = -\frac{1}{2}\left(c_x(u)R + c(u)S_x\right), \\ u_t = \frac{R+S}{2}, \end{cases} \tag{2.9}$$

which can be obtained from (2.6) using the product rules

$$(c(u)R)_x = c_x(u)R + c(u)R_x, \quad (c(u)S)_x = c_x(u)S + c(u)S_x.$$

Based on this, we propose the following energy conservative scheme

$$\begin{aligned} &(R_j)_t - \frac{1}{2}D^0\left(c_j R_j\right) = \frac{1}{2}\left(D^0 c_j S_j + c_j D^0 R_j\right), \\ &(S_j)_t + \frac{1}{2}D^0\left(c_j S_j\right) = -\frac{1}{2}\left(D^0 c_j R_j + c_j D^0 S_j\right), \\ &(u_j)_t = \frac{R_j + S_j}{2}. \end{aligned} \tag{2.10}$$

The scheme satisfies the following discrete energy identity:

**Lemma 2.3.** *Let $R_j(t)$ and $S_j(t)$ be approximate solutions generated by the scheme (2.10). Then*

$$\frac{d}{dt}\left(\frac{h}{2}\sum_j (R_j^2(t) + S_j^2(t))\right) = 0.$$

*Proof.* To prove this lemma, we multiply the first equation in (2.10) by $R_j$ and the second by $S_j$, add them up and sum over all the indices $j$. We obtain

$$\frac{1}{2}\frac{d}{dt}\sum_j \left(R_j^2 + S_j^2\right) = \frac{1}{2}\sum_j \left(R_j D^0\left(c_j R_j\right) + c_j R_j D^0 R_j - S_j D^0\left(c_j S_j\right) - c_j S_j D^0 S_j\right).$$

Renaming indices in the terms on the right hand side of this equation and using the boundary conditions, we realize it is equal to zero.

□

2.7. **Energy dissipating scheme based on the Riemann invariants formulation.** In order to approximate dissipative solutions, we add numerical viscosity to the energy conservative scheme (2.10) to obtain,

$$\begin{aligned} &(R_j)_t - \frac{1}{2}D^0\left(c_j R_j\right) = \frac{1}{2}\left(D^0 c_j S_j + c_j D^0 R_j\right) + \frac{h}{2}D^-\left(s_{j+\frac{1}{2}} D^+ R_j\right), \\ &(S_j)_t + \frac{1}{2}D^0\left(c_j S_j\right) = -\frac{1}{2}\left(D^0 c_j R_j + c_j D^0 S_j\right) + \frac{h}{2}D^-\left(s_{j+\frac{1}{2}} D^+ S_j\right), \\ &(u_j)_t = \frac{R_j + S_j}{2}, \end{aligned} \tag{2.11}$$

where we have chosen $s_{j\pm\frac{1}{2}} = \max\{c_j, c_{j\pm1}\}$, the maximum local wave speed.

We have the following lemma illustrating the energy dissipation associated with (2.11):

**Lemma 2.4.** *Let $R_j(t)$ and $S_j(t)$ be approximate solutions generated by the scheme (2.11). Then,*

$$\frac{d}{dt}\left(\frac{h}{2}\sum_j (R_j^2(t) + S_j^2(t))\right) \leq 0,$$

*where the inequality is strict if $R$ or $S$ is not constant.*

The proof of this lemma is similar to the proof of Lemma 2.2 and is therefore omitted.

## 3. Numerical experiments

In this section, we will test the numerical schemes developed in the previous section on specific numerical examples.

3.1. **Notation.** For convenience, we will use the following abbreviations for the schemes: The schemes in the variables $v$ and $w$, (2.3) and (2.4), will be denoted 'vwc' and 'vwd' respectively ('c' for conservative and 'd' for dissipative). The schemes in the variables $R$ and $S$, (2.10) and (2.11), will be denoted 'RSc' and 'RSd' respectively.

3.2. **Time stepping.** As the schemes (2.3), (2.4), (2.10) and (2.11) are semi-discrete, we need to use a suitable time integrator to compute approximations. For the energy-conservative schemes, we use a midpoint rule, which looks as follows in the case of scheme (2.3):

$$\begin{aligned} D_t v_j^n &= c_j^n D^0 w_j^{n+1/2}, \\ D_t w_j^n &= D^0 \left( c_j^n v_j^{n+1/2} \right), \\ D_t u_j^n &= v_j^n, \end{aligned} \tag{3.1}$$

We denoted $v_j^{n+1/2} = (v_j^n + v_j^{n+1})/2$ the average of the approximation at time $t_n$ and time $t_{n+1}$ and similarly for $w_j^{n+1/2}$. Alternatively one could stagger $u$ with respect to the other variables $v$ and $w$. We have:

**Lemma 3.1.** *The time integration as in (3.1) preserves a discrete version of the energy (2.2) in every time step, that is,*

$$\frac{h}{2} \sum_j \left(v_j^{n+1}\right)^2 + \left(w_j^{n+1}\right)^2 = \frac{h}{2} \sum_j \left(v_j^n\right)^2 + \left(w_j^n\right)^2$$

*for any $n \geq 0$.*

*Proof.* Multiplying the first equation in (3.1) by $v_j^{n+1/2}$ and the second by $w_j^{n+1/2}$ , adding up and summing over all $j$, one can see that the scheme preserves a time discrete version of the energy in Lemma 2.1. □

In a similar manner, we integrate the conservative scheme in the $R$ and $S$ variables, (2.10), and obtain a fully discrete energy-conserving scheme.

For the energy-dissipative schemes we use a third order SSP-Runge Kutta method (RK-SSP), see [15].

3.3. **Gaussian pulse.** As a test problem we consider (1.3) with the initial data

$$\begin{aligned} u_0(x) &= \frac{\pi}{4} + \exp(-x^2), \\ u_1(x) &= -c(u_0(x))\,(u_0)_x(x), \end{aligned} \tag{3.2}$$

on the domain $D = [-15, 15]$ with periodic boundary conditions and the function $c(u)$ given by

$$c(u) = \sqrt{\alpha \cos^2(u) + \beta \sin^2(u)}, \tag{3.3}$$

where $\alpha, \beta$ are positive constants. For this experiment, we choose $\alpha = 0.5$ and $\beta = 4.5$. This Cauchy problem has already been numerically investigated in [12] and [16], however with different coefficients $\alpha$ and $\beta$. Since we did not observe a dichotomy of dissipative and conservative solutions for the values of the coefficients taken there, we will use $\alpha = 0.5$ and $\beta = 4.5$ here. We compute approximations by the schemes at times, $T = 1, 5, 10$. In Figure 3.1 the approximations computed by schemes (2.3) and (2.4) at times $T = 1, 5, 10$ are shown. We observe that at time $T = 1$ the approximated solution appears smooth whereas at time $T = 10$, we observe kinks in the solution indicating that singularities have appeared by this time.

Since the schemes (2.3) and (2.4) are based on the first-order system (2.1), we plot the quantities $v$ and $w$ in Figures 3.2 and 3.3. We observe high frequency oscillations in the approximations computed by the energy-conservative scheme (2.3). This is not unexpected as there is no numerical viscosity in these approximations and the high frequency oscillations are a manifestation of this effect. Furthermore, at time $T = 1$, the two approximations computed by (2.3) and (2.4) look alike, whereas we observe visible differences at time $T = 10$.

Similarly, the approximations computed with scheme (2.10) are qualitatively very close to those computed by the energy conservative scheme (2.3), whereas the approximations computed with (2.11) resemble those computed with (2.4). Furthermore, as predicted by our analysis and shown in Figure 3.4, the conservative schemes almost preserve the discrete $L^2$-energy over time whereas the approximations computed by the dissipative schemes lose energy by a significant amount.

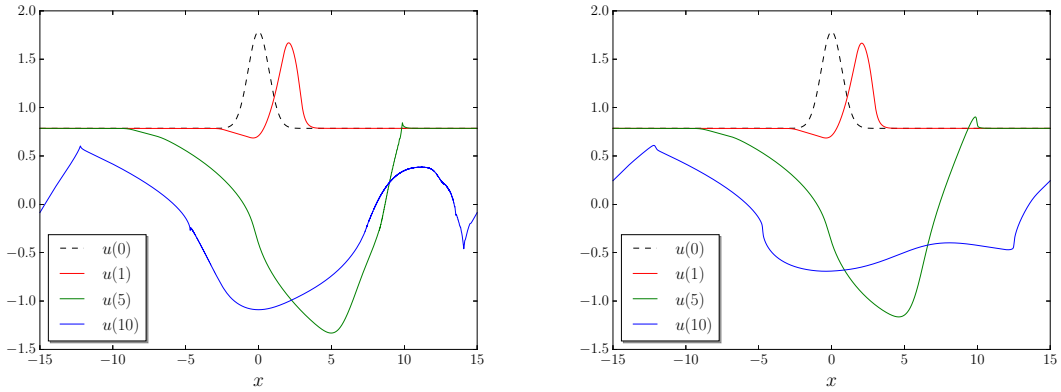


FIGURE 3.1. Approximations of $u$ in (1.3), (3.2), (3.3) computed by scheme (2.3) and scheme (2.4) on a grid with $N = 2^{14}$ points at time $T = 0, 1, 5, 10$. Left: Approximation by energy-conservative scheme (2.3), Right: Approximation by energy-dissipative scheme (2.4).

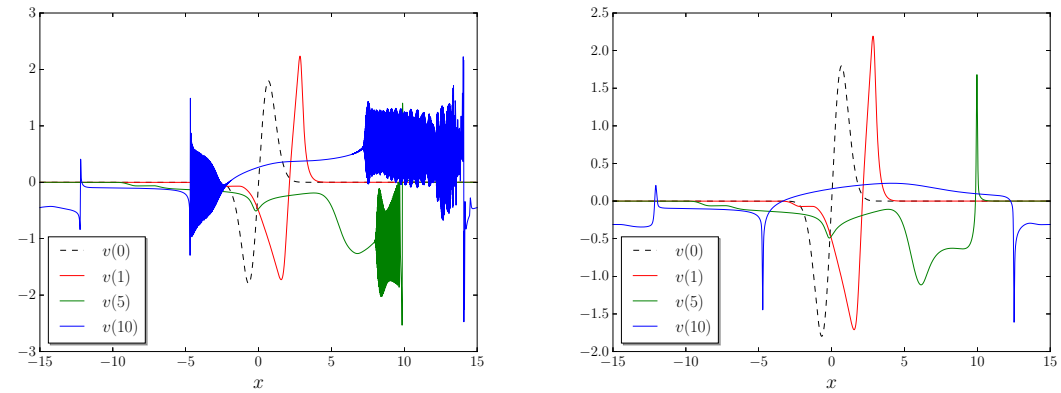


FIGURE 3.2. Approximations of the quantity $v$ in (2.1), (3.2), (3.3) computed by scheme (2.3) and scheme (2.4) on a grid with $N = 2^{14}$ points at time $T = 0, 1, 5, 10$. Left: Approximation by scheme (2.3), Right: Approximation by scheme (2.4).

To investigate the possibility of different limit solutions approximated by the conservative and dissipative schemes, we compute reference approximations with schemes (2.3) and (2.4) at times $T = 1, 10$, on a grid with $N = 2^{14}$ points and test the convergence of the schemes towards these reference solutions. We measure the distance to the reference solutions in the following discrete relative $L^2$-norm,

$$\|\mathbf{a} - \mathbf{b}\|_{\ell^2_{rel}} := \frac{\left(\sum_j (a_j - b_j)^2\right)^{1/2}}{\left(\sum_j (a_j)^2\right)^{1/2} + \left(\sum_j (b_j)^2\right)^{1/2}} \tag{3.4}$$

for vectors $\mathbf{a} = (\dots, a_{j-1}, a_j, a_{j+1}, \dots)$, $\mathbf{b} = (\dots, b_{j-1}, b_j, b_{j+1}, \dots)$. The distances to the conservative and dissipative reference solution respectively, are shown in Plots 3.5 and 3.6.

We note that at time $T = 1$, all approximations to the variable $u$ seem to converge to both reference solutions, which means that the two reference solutions are very close to each other. The convergence rates are approximately 1 which is what we expect for smooth solutions due to the formal order 1 of the schemes (this can be found via a truncation error analysis).

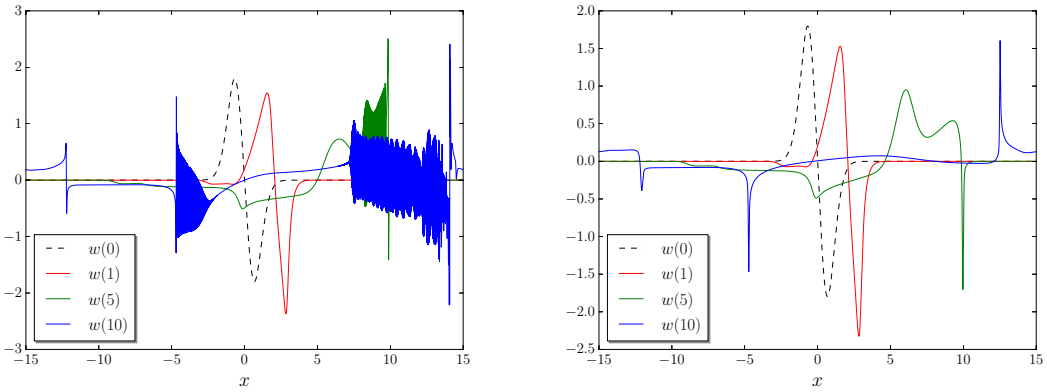


FIGURE 3.3. Approximations of the quantity $w$ in (2.1), (3.2), (3.3) computed by scheme (2.3) and scheme (2.4) on a grid with $N = 2^{14}$ points at time $T = 0, 1, 5, 10$. Left: Approximation by scheme (2.3), Right: Approximation by scheme (2.4).

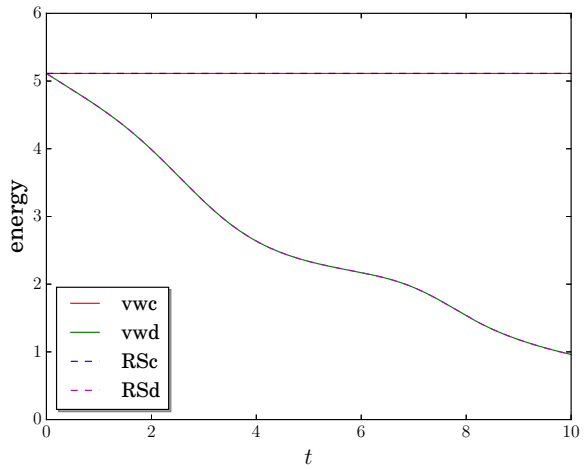


FIGURE 3.4. Evolution of discrete energies over time, $N = 2^{11}$.

However, at time $T = 10$, the approximations of the conservative schemes still seem to be converging to the reference solution computed by (2.3) whereas no convergence can be observed for the energy dissipative schemes (2.4) and (2.11). Similarly, the dissipative schemes seem to be converging to the dissipative reference solution whereas the distance of the conservative approximations computed by (2.3) and (2.10) to the dissipative reference solution remains (approximately) constant despite mesh refinement. The convergence rates for the respective convergent schemes are lower compared to those at time $T = 1$ which can be explained by the singularity formation and decreased regularity of the solutions.

We conclude that the energy-conservative schemes converge to a different limit solution than the energy-dissipative schemes in this example. Furthermore, as the conservative schemes preserve energy, the limit of these schemes is the conservative solution. Similarly, the dissipative schemes converge to a solution that has lower energy than the initial data. Hence, this solution appears to be a dissipative solution of (1.3).

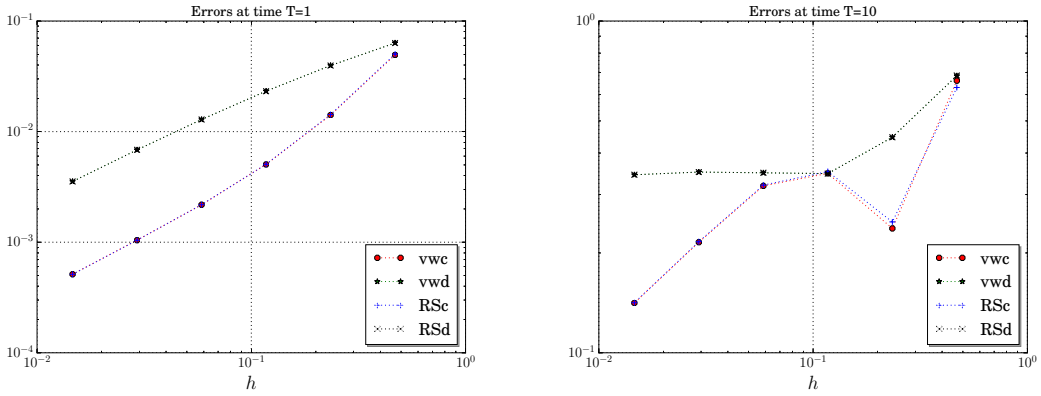


FIGURE 3.5. $\|\mathbf{u}_h - \mathbf{u}_{\text{ref}}\|_{\ell^2_{rel}}$ for different mesh resolutions, $T = 1, 10$, $\mathbf{u}_h$ approximation computed by the various schemes at different mesh resolutions, $\mathbf{u}_{\text{ref}}$ the reference solution computed by scheme (2.3) (with $N = 2^{14}$).

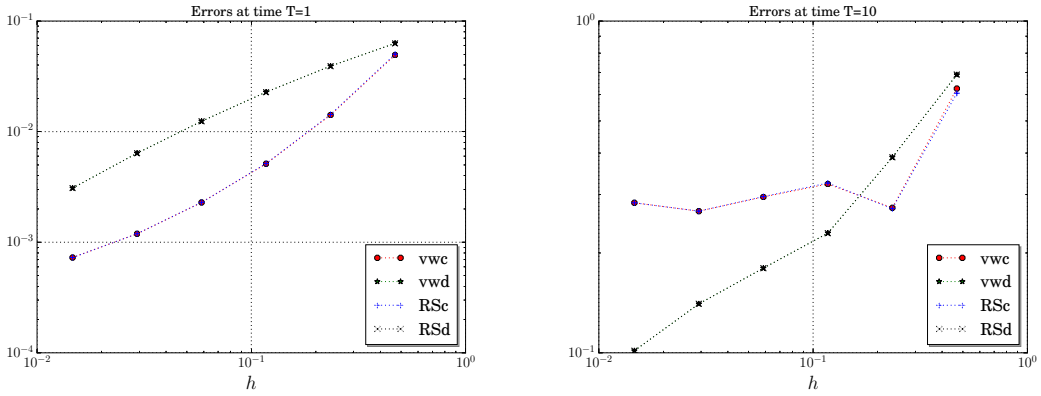


FIGURE 3.6. $\|\mathbf{u}_h - \mathbf{u}_{\text{ref}}\|_{\ell^2_{rel}}$ for different mesh resolutions, $T = 1, 10$, $\mathbf{u}_h$ approximation computed by the various schemes at different mesh resolutions, $\mathbf{u}^N_{\text{ref}}$ the dissipative reference solution computed by scheme (2.4) (on a grid with $N = 2^{14}$ points).

3.4. **Multiplicity of dissipative solutions?** The above numerical experiments clearly illustrate that one set of schemes converges to a conservative solution whereas another converges to a dissipative solution of the variational wave equation (1.3). Is there uniqueness within these two classes of solutions? A priori, one might guess that in contrast to conservative solutions, one might be able to construct multiple dissipative solutions by varying the amount and rate of energy dissipation. We study this possibility by modifying the dissipative scheme (2.4) to

$$\begin{aligned} (v_j)_t - c_j D^0 w_j &= \frac{h\,\kappa}{2} D^- \left( s_{j+\frac{1}{2}} D^+ v_j \right) \\ (w_j)_t - D^0 \left( c_j v_j \right) &= \frac{h\,\kappa}{2} D^- \left( s_{j+\frac{1}{2}} D^+ w_j \right), \\ (u_j)_t &= v_j, \end{aligned} \tag{3.5}$$

by adding $\kappa$ to scale the numerical viscosity in (2.4)[1]. We investigate the above question by setting $\kappa$ to different values, resulting in different amounts of energy-loss and possibly, convergence to different dissipative solutions. We test the convergence of the resulting numerical approximations

[1] In a similar way, we generalize scheme (2.11).

of (1.3), (3.2), (3.3) by scheme (3.5) for $\kappa = 0.01, 0.05, 0.1, 1, 2, 5, 10$ towards the reference solutions from Section 3.3, computed by both schemes (2.3) and (2.4). The distance to the reference as defined in (3.4) are displayed in Figure 3.7 (dissipative reference solution) for time $T = 10$ (after singularity formation).

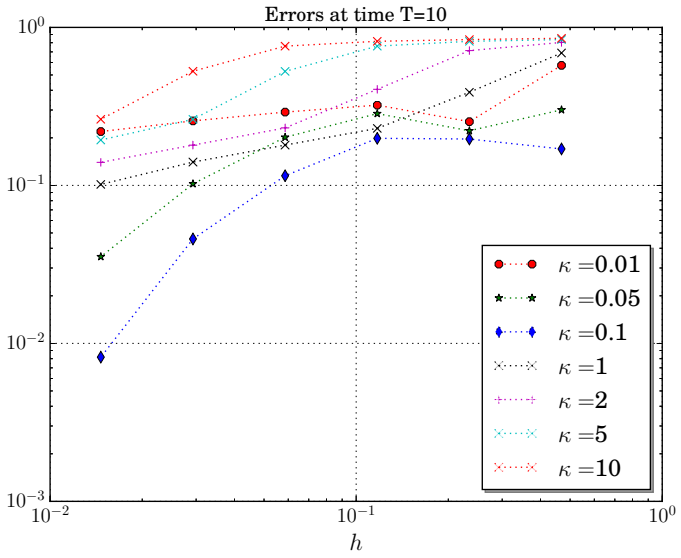


FIGURE 3.7. $\|\mathbf{u}_h - \mathbf{u}_{\text{ref}}\|_{\ell^2_{rel}}$ between the dissipative reference solution computed by (2.4) and the approximations by (3.5) for different mesh resolutions and diffusion coefficient $\kappa$, $T = 10$.

The results, presented in Figure 3.7, show that all the approximations (computed with different values of the diffusion coefficient $\kappa$), clearly converge to the same dissipative reference solution. Furthermore, we have listed the discrete energy ratio

$$E_{\text{rel}} = \frac{\sum_j \{(v_j^M)^2 + (w_j^M)^2\}}{\sum_j \{(v_j^0)^2 + (w_j^0)^2\}}, \tag{3.6}$$

where $v_j^0$, $w_j^0$ are the approximations at the initial time and $v_j^M$, $w_j^M$ are the approximations at the final time $T$. From Table 3.1, we observe that these ratios seem to converge to $\approx 0.2$ for all the tested $\kappa$, showing that there is a universal rate of energy dissipation associated with the dissipative solutions (at least in this example).

| $h \setminus \kappa$ | 0.01 | 0.05 | 0.1 | 1 | 2 | 5 | 10 |
|---|---|---|---|---|---|---|---|
| $2^{-2}$ | 0.844 | 0.500 | 0.333 | 0.074 | 0.026 | 0.005 | 0.001 |
| $2^{-3}$ | 0.802 | 0.490 | 0.312 | 0.129 | 0.070 | 0.017 | 0.005 |
| $2^{-4}$ | 0.709 | 0.376 | 0.251 | 0.163 | 0.127 | 0.052 | 0.017 |
| $2^{-5}$ | 0.617 | 0.294 | 0.21 | 0.178 | 0.162 | 0.110 | 0.051 |
| $2^{-6}$ | 0.530 | 0.237 | 0.203 | 0.184 | 0.177 | 0.153 | 0.109 |
| $2^{-7}$ | 0.422 | 0.212 | 0.204 | 0.189 | 0.184 | 0.173 | 0.153 |
| $2^{-8}$ | 0.333 | 0.208 | 0.205 | 0.194 | 0.189 | 0.182 | 0.173 |
| $2^{-9}$ | 0.280 | 0.208 | 0.206 | 0.199 | 0.194 | 0.187 | 0.182 |

TABLE 3.1. $E_{\text{rel}}$ as in (3.6) for different mesh resolutions and diffusion coefficient $\kappa$, $T = 10$.

## 4. Numerical schemes in two-space dimensions

As in the one-dimensional case, we will design energy conservative and energy dissipative finite difference discretizations of the two-dimensional version of the nonlinear variational wave equation (1.7) by rewriting it as a first-order system. To this end, we introduce three new independent variables:

$$\begin{aligned} p &:= u_t, \\ v &:= \cos(u)u_x + \sin(u)u_y, \\ w &:= \sin(u)u_x - \cos(u)u_y. \end{aligned}$$

Then, for smooth solutions, equation (1.7) is equivalent to the following system for $(p, v, w, u)$,

$$\begin{cases} p_t - \alpha(\phi(u)v)_x - \alpha(\psi(u)v)_y - \beta(\psi(u)w)_x + \beta(\phi(u)w)_y - \alpha vw + \beta vw = 0, \\ v_t - \phi(u)p_x - \psi(u)p_y + pw = 0, \\ w_t - \psi(u)p_x + \phi(u)p_y - pv = 0, \\ u_t = v \end{cases} . \tag{4.1}$$

where $\phi(u) := \cos(u)$, and $\psi(u) := \sin(u)$.

4.1. **The grid.** We introduce some notation needed to define the finite difference schemes in two space dimensions. We reserve $h$ and $\Delta t$ to denote two small positive numbers that represent the spatial and temporal discretization parameters, respectively, of the numerical schemes. For $i$, $j \in \mathbb{Z}$, we set $x_i = ih$, $y_j = jh$ and for $n = 0, 1, ..., N$, where $N\Delta t = T$ for some fixed time horizon $T > 0$, we set $t_n = n\Delta t$. For any function $g = g(x, y)$, we write $g_{i,j} = g(x_i, y_j)$, and similarly for any function $g = g(x, y, t)$, we write $g^n_{i,j} = g(x_i, y_j, t_n)$. We also introduce the Cartesian spatial and temporal grid cells

$$I_{i,j} = [x_{i-\frac{1}{2}}, x_{i+\frac{1}{2}}) \times [y_{j-\frac{1}{2}}, y_{j+\frac{1}{2}}), \qquad I^n_{i,j} = I_{i,j} \times [t_n, t_{n+1}).$$

We will use the following finite difference operators

$$\begin{aligned} D^{\pm}_x \rho_{i,j} &= \pm \frac{\rho_{i\pm1,j} - \rho_{i,j}}{h}, \quad D^0_x \rho_{i,j} = \frac{1}{2}\left(D^+_x + D^-_x\right)\rho_{i,j}, \\ D^{\pm}_y \rho_{i,j} &= \pm \frac{\rho_{i,j\pm1} - \rho_{i,j}}{h}, \quad D^0_y \rho_{i,j} = \frac{1}{2}\left(D^+_y + D^-_y\right)\rho_{i,j}. \end{aligned}$$

4.2. **Energy conservative scheme.** Based on the first order system (4.1), we propose the following semi-discrete difference scheme to approximate the two-dimensional version of the nonlinear variational wave equation (1.7):

$$\begin{aligned} &(p_{i,j})_t - \alpha D^0_x\left(\phi_{i,j}v_{i,j}\right) - \alpha D^0_y\left(\psi_{i,j}v_{i,j}\right) - \beta D^0_x\left(\psi_{i,j}w_{i,j}\right) + \beta D^0_y\left(\phi_{i,j}w_{i,j}\right) \\ &\qquad\qquad - \alpha v_{i,j}\, w_{i,j} + \beta v_{i,j}\, w_{i,j} = 0, \\ &(v_{i,j})_t - \phi_{i,j} D^0_x p_{i,j} - \psi_{i,j} D^0_y p_{i,j} + p_{i,j} w_{i,j} = 0, \\ &(w_{i,j})_t - \psi_{i,j} D^0_x p_{i,j} + \phi_{i,j} D^0_y p_{i,j} - p_{i,j} v_{i,j} = 0, \\ &(u_{i,j})_t = v_{i,j}. \end{aligned} \tag{4.2}$$

The above scheme preserves a discrete version of the energy as reported in the following lemma:

**Lemma 4.1.** *Let $p_{i,j}(t)$, $v_{i,j}(t)$ and $w_{i,j}(t)$ be approximate solutions generated by the scheme (4.2). Then*

$$\frac{d}{dt}\left(\frac{h^2}{2}\sum_i\sum_j (p^2_{i,j}(t) + \alpha\, v^2_{i,j}(t) + \beta\, w^2_{i,j}(t))\right) = 0.$$

The proof of this lemma is analogous to the proof of Lemma 2.1.

4.3. **Energy dissipative scheme.** As in the one-dimensional case, we can add some *numerical viscosity* to the energy conservative scheme (4.2) to obtain the following energy dissipative scheme for approximating the variational wave equation (1.7):

$$
\begin{aligned}
&(p_{i,j})_t - \alpha D_x^0\left(\phi_{i,j} v_{i,j}\right) - \alpha D_y^0\left(\psi_{i,j} v_{i,j}\right) - \beta D_x^0\left(\psi_{i,j} w_{i,j}\right) + \beta D_y^0\left(\phi_{i,j} w_{i,j}\right) \\
&\qquad - \alpha v_{i,j}\, w_{i,j} + \beta v_{i,j}\, w_{i,j} = \frac{\nu h}{2} D_x^- D_x^+ p_{i,j} + \frac{\nu h}{2} D_y^- D_y^+ p_{i,j}, \\
&(v_{i,j})_t - \phi_{i,j} D_x^0 p_{i,j} - \psi_{i,j} D_y^0 p_{i,j} + p_{i,j} w_{i,j} = \frac{\nu h}{2} D_x^- D_x^+ v_{i,j} + \frac{\nu h}{2} D_y^- D_y^+ v_{i,j}, \\
&(w_{i,j})_t - \psi_{i,j} D_x^0 p_{i,j} + \phi_{i,j} D_y^0 p_{i,j} - p_{i,j} v_{i,j} = \frac{\nu h}{2} D_x^- D_x^+ w_{i,j} + \frac{\nu h}{2} D_y^- D_y^+ w_{i,j}, \\
&(u_{i,j})_t = v_{i,j}.
\end{aligned}
\tag{4.3}
$$

where $\nu > 0$ is a constant. Alternatively, one could choose $\nu$ varying in space and depending on the wave speeds as we did in the one dimensional case.

Following similar arguments to those used in the proof of Lemma 2.2, one can show:

**Lemma 4.2.** *Let $p_{i,j}(t)$, $v_{i,j}(t)$ and $w_{i,j}(t)$ be approximate solutions generated by the scheme (4.3). Then*

$$
\frac{d}{dt}\left(\frac{h^2}{2}\sum_i\sum_j (p_{i,j}^2(t) + \alpha\, v_{i,j}^2(t) + \beta\, w_{i,j}^2(t))\right) \le 0,
$$

*with equality if and only if $p$, $v$, and $w$ are constant.*

4.4. **Numerical experiments.** We illustrate the energy conservative scheme (4.2) and the energy dissipative scheme (4.3) by considering the first-order system (4.1) with the following initial data

$$
u_0(x,y) = 2\cos(2\pi x)\sin(2\pi y), \tag{4.4a}
$$

$$
u_1(x,y) = \sin(2\pi(x-y)), \tag{4.4b}
$$

on the domain $D = [0,1]^2$ with periodic boundary conditions and coefficients $\alpha = 0.5$, $\beta = 1.5$ in $a$, $b$ and $c$ at times $T = 2$ and $T = 4$. For the time integration we again use a third order strong stability preserving Runge Kutta method for the energy dissipative scheme and leap frog time stepping for the energy conservative scheme.

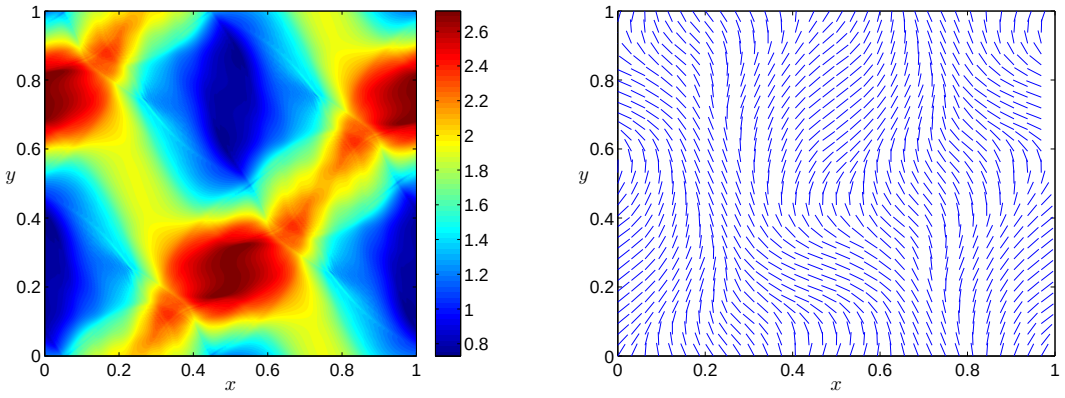


FIGURE 4.1. Approximations of the solution of (1.7) computed by scheme (4.2) on a grid with cell size $h = \Delta y = 2^{-11}$, CFL-number $\theta = 0.4$ at time $T = 2$. Left: the angle $u$, Right: the corresponding director $\mathbf{n} = (\cos(u), \sin(u))$.

Approximations computed by schemes (4.2), (4.3) respectively, on a mesh with 2048 points in each coordinate direction can be seen in Figures 4.1, 4.2, 4.3 and 4.4. From the above figures,

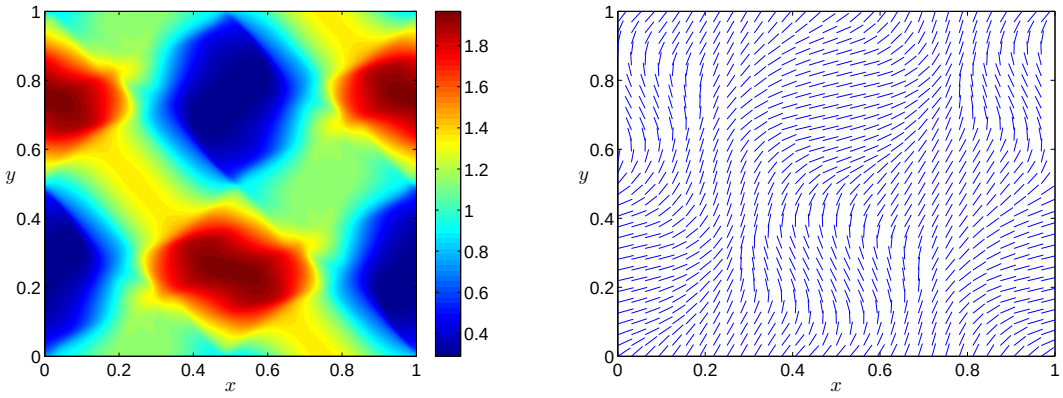


FIGURE 4.2. Approximations of the solution of (1.7) computed by scheme (4.3) on a grid with cell size $h = 2^{-11}$ at time $T = 2$. Left: the angle $u$, Right: the corresponding director $\mathbf{n} = (\cos(u), \sin(u))$.

we observe that both the conservative and dissipative schemes seem to resolve the solution in a stable manner. Although the two schemes seems to converge to the same limit at time $T = 2$, the limits, computed by the energy conservative and energy dissipative schemes differ at time $T = 4$. These results are also confirmed by a convergence study, performed in a manner analogous to the one-dimensional case. However, we omit the convergence tables for brevity.

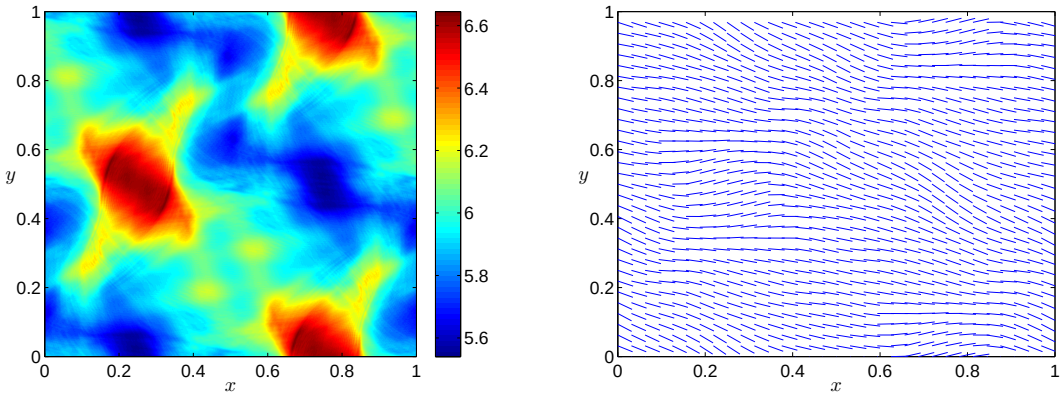


FIGURE 4.3. Approximations of the solution of (1.7) computed by scheme (4.2) on a grid with cell size $h = 2^{-11}$ at time $T = 4$. Left: the angle $u$, right: the corresponding director $\mathbf{n} = (\cos(u), \sin(u))$.

## 5. CONCLUSION

We have considered a nonlinear variational wave equation, that models (both one and two dimensional) planar waves in the dynamics of nematic liquid crystals. Our schemes are based on either the conservation or the dissipation of the energy associated with these equations. In the one-dimensional case, we rewrite the variational wave equation (1.3) in the form of two equivalent first-order systems. Energy conservative as well as energy dissipative schemes, approximating both these formulations are derived. Numerical experiments performed with these schemes strongly suggest

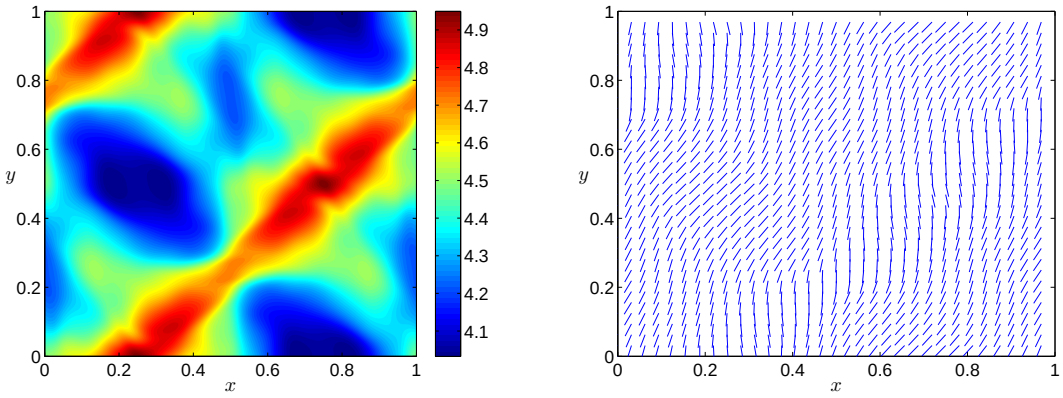


FIGURE 4.4. Approximations of the solution of (1.7) computed by scheme (4.3) on a grid with cell size $h = 2^{-11}$ at time $T = 4$. Left: the angle $u$, right: the corresponding director $\mathbf{n} = (\cos(u), \sin(u))$.

(1) All the designed schemes resolve the solution (including possible singularities in the angle $u$) in a stable manner.
(2) The energy conservative schemes converge to a limit solution (as the mesh is refined), whose energy is preserved. This solution is a *conservative* solution of (1.3).
(3) The energy dissipative schemes also converge to a limit solution with energy being dissipated with time. This solution is a *dissipative* solution of the variational wave equation. Furthermore, this dissipative solution appears to be unique. Varying the amount of numerical viscosity does not affect the limiting rate of entropy dissipation.

We also design both energy conservative as well as energy dissipative finite difference schemes for the two-dimensional version of the variational wave equation (1.7) based on the first-order system (4.1). Again, these schemes approximate the conservative, resp. dissipative, solutions efficiently.

Thus, we have designed a stable, simple to implement, set of finite difference schemes that can approximate both the conservative as well as the dissipative solutions of the nonlinear variational wave equations. These schemes will be utilized in a forthcoming paper to study realistic modeling scenarios involving liquid crystals.

## REFERENCES

[1] *Variational Methods: Proceedings of a Conference Paris, June 1988*. Progress in Nonlinear Differential Equations and Their Applications. Birkhäuser Boston, 2012.
[2] G. Alì and J. K. Hunter. Orientation waves in a director field with rotational inertia. *Kinet. Relat. Models*, 2(1):1–37, 2009.
[3] S. Badia, F. Guillén-González, and J. V. Gutiérrez-Santacreu. Finite element approximation of nematic liquid crystal flows using a saddle-point structure. *J. Comput. Phys.*, 230(4):1686–1706, 2011.
[4] S. Badia, F. Guillén-Gónzalez, and J. V. Gutiérrez-Santacreu. An overview on numerical analyses of nematic liquid crystal flows. *Arch. Comput. Methods Eng.*, 18(3):285–313, 2011.
[5] S. Bartels and A. Prohl. Constraint preserving implicit finite element discretization of harmonic map flow into spheres. *Math. Comp.*, 76(260):1847–1859 (electronic), 2007.
[6] R. Becker, X. Feng, and A. Prohl. Finite element approximations of the Ericksen-Leslie model for nematic liquid crystal flow. *SIAM J. Numer. Anal.*, 46(4):1704–1731, 2008.
[7] A. Bressan and Y. Zheng. Conservative solutions to a nonlinear variational wave equation. *Comm. Math. Phys.*, 266(2):471–497, 2006.
[8] D. Christodoulou and A. S. Tahvildar-Zadeh. On the regularity of spherically symmetric wave maps. *Comm. Pure Appl. Math.*, 46(7):1041–1091, 1993.
[9] J. Coron, J. Ghidaglia, and F. Hélein. *Nematics: mathematical and physical aspects*. NATO ASI series: Mathematical and physical sciences. Kluwer Academic, 1991.
[10] R. J. DiPerna and A. J. Majda. Oscillations and concentrations in weak solutions of the incompressible fluid equations. *Comm. Math. Phys.*, 108(4):667–689, 1987.

[11] J. Ericksen and D. Kinderlehrer. *Theory and Applications of Liquid Crystals*. The IMA Volumes in Mathematics and its Applications. Springer New York, 2012.
[12] R. Glassey, J. Hunter, and Y. Zheng. Singularities and oscillations in a nonlinear variational wave equation. In J. Rauch and M. Taylor, editors, *Singularities and Oscillations*, volume 91 of *The IMA Volumes in Mathematics and its Applications*, pages 37–60. Springer New York, 1997.
[13] R. T. Glassey. Finite-time blow-up for solutions of nonlinear wave equations. *Math. Z.*, 177(3):323–340, 1981.
[14] R. T. Glassey, J. K. Hunter, and Y. Zheng. Singularities of a variational wave equation. *J. Differential Equations*, 129(1):49–78, 1996.
[15] S. Gottlieb, C.-W. Shu, and E. Tadmor. Strong stability-preserving high-order time discretization methods. *SIAM Rev.*, 43(1):89–112 (electronic), 2001.
[16] H. Holden, K. H. Karlsen, and N. H. Risebro. A convergent finite-difference method for a nonlinear variational wave equation. *IMA J. Numer. Anal.*, 29(3):539–572, 2009.
[17] H. Holden and X. Raynaud. Global semigroup of conservative solutions of the nonlinear variational wave equation. *Arch. Ration. Mech. Anal.*, 201(3):871–964, 2011.
[18] T. K. Karper and F. Weber. A new angular momentum method for computing wave maps into spheres. *SIAM J. Numer. Anal.*, 52(4):2073–2091, 2014.
[19] F. M. Leslie. Theory of flow phenomena in nematic liquid crystals. In J. Ericksen and D. Kinderlehrer, editors, *Theory and Applications of Liquid Crystals*, volume 5 of *The IMA Volumes in Mathematics and Its Applications*, pages 235–254. Springer New York, 1987.
[20] F.-H. Lin and C. Liu. Nonparabolic dissipative systems modeling the flow of liquid crystals. *Comm. Pure Appl. Math.*, 48(5):501–537, 1995.
[21] F.-H. Lin and C. Liu. Existence of solutions for the Ericksen-Leslie system. *Arch. Ration. Mech. Anal.*, 154(2):135–156, 2000.
[22] V. Lisin and A. Potapov. Nonlinear interaction between acoustic and orientation waves in liquid crystals. *Radiophysics and Quantum Electronics*, 38(1-2):98–101, 1995.
[23] R. A. Saxton. Dynamic instability of the liquid crystal director. In *Current progress in hyperbolic systems: Riemann problems and computations (Brunswick, ME, 1988)*, volume 100 of *Contemp. Math.*, pages 325–330. Amer. Math. Soc., Providence, RI, 1989.
[24] J. Shatah. Weak solutions and development of singularities of the SU(2) $\sigma$-model. *Comm. Pure Appl. Math.*, 41(4):459–469, 1988.
[25] J. Shatah and A. Tahvildar-Zadeh. Regularity of harmonic maps from the Minkowski space into rotationally symmetric manifolds. *Comm. Pure Appl. Math.*, 45(8):947–971, 1992.
[26] V. A. Vladimirov and M. Y. Zhukov. Vibrational fréedericksz transition in liquid crystals. *Phys. Rev. E*, 76:031706, Sep 2007.
[27] P. Zhang and Y. Zheng. On oscillations of an asymptotic equation of a nonlinear variational wave equation. *Asymptot. Anal.*, 18(3-4):307–327, 1998.
[28] P. Zhang and Y. Zheng. Rarefactive solutions to a nonlinear variational wave equation of liquid crystals. *Comm. Partial Differential Equations*, 26(3-4):381–419, 2001.
[29] P. Zhang and Y. Zheng. Singular and rarefactive solutions to a nonlinear variational wave equation. *Chinese Ann. Math. Ser. B*, 22(2):159–170, 2001.
[30] P. Zhang and Y. Zheng. Weak solutions to a nonlinear variational wave equation. *Arch. Ration. Mech. Anal.*, 166(4):303–319, 2003.
[31] P. Zhang and Y. Zheng. On the global weak solutions to a variational wave equation. In *Evolutionary equations. Vol. II*, Handb. Differ. Equ., pages 561–648. Elsevier/North-Holland, Amsterdam, 2005.
[32] P. Zhang and Y. Zheng. Weak solutions to a nonlinear variational wave equation with general data. *Ann. Inst. H. Poincaré Anal. Non Linéaire*, 22(2):207–226, 2005.

(F. Weber)
Seminar for Applied Mathematics, ETH Zürich, 8092 Zürich, Switzerland.
*E-mail address*: franziska.weber@sam.math.ethz.ch